Journal of Alloys and Compounds 509 (2011) 9466–9471

Contents lists available at ScienceDirect

Journal of Alloys and Compounds

journal homepage: www.elsevier.com/locate/jallcom

Study of the temperature and organic bindings effects in the dielectric and structural properties of the lithium ferrite ceramic matrix ($LiFe_5O_8$)

M.M. Costa[a,d,*], R.S.T.M. Sohn[a,b], A.A.M. Macêdo[c], S.E. Mazzetto[c], M.P.F. Graça[e], A.S.B. Sombra[a,b]

[a] Telecommunications and Materials Science and Engineering Laboratory (LOCEM), Department of Physics, Federal University of Ceará, Campus do Pici, Postal Code 6030, 60455-760 Fortaleza, CE, Brazil
[b] Department of Physics, Federal University of Ceará, Campus do Pici, Postal Code 6030, 60455-760 Fortaleza, CE, Brazil
[c] Technology Products Laboratory (LPT), Northeast Network on Biotechnology (RENORBIO), Federal University of Ceará, Postal Code 6021, 60455-900 Fortaleza, CE, Brazil
[d] Department of Physics, Federal University of Mato Grosso – UFMT, 78060-900 Cuiabá, MT, Brazil
[e] I3N – Aveiro, Physics Department, Aveiro University, Campus Universitário de Santiago, 3810-193, Aveiro, Portugal

ARTICLE INFO

Article history:
Received 12 March 2011
Received in revised form 13 July 2011
Accepted 14 July 2011
Available online 30 July 2011

Keywords:
Ceramic
Lithium ferrite
Magnetic material
Dielectric spectroscopy

ABSTRACT

In this study, the effects of the calcination temperature and of the organic bindings in the structural and dielectric properties of lithium ferrite ($LiFe_5O_8$) were investigated. The organic bindings used were glycerol, PVA (polyvinyl alcohol) and Galactomannan (*Adenanthera pavonina*). The investigated calcination temperature range was from 773 K to 1073 K. The structural properties were analyzed using differential scanning calorimetry, thermogravimetry, X-ray diffraction and infra-red spectroscopy. The electrical and magnetical properties were investigated using impedance dielectric spectroscopy and Mössbauer spectroscopy. The study of the structural and electrical properties of the lithium ferrites is an important issue in view to their attractive technological properties and low cost of fabrication. This work shows that the binding type, affects significantly the dielectric constant and loss of the $LiFe_5O_8$ ceramics.

1. Introduction

In solid state materials, mixed spinel ferrites have gained a prime importance because of their various potential applications. One example of this mixed spinel is the lithium and substituted lithium ferrites, which present actually high scientific and technological interest due to their attractive physical properties like the high Curie temperature, the presence of a hysteresis loop, high saturation magnetization and good thermal stability. Due to these properties, potential technological applications as, for example, cathode materials in lithium ion batteries [1–3] and microwave applications [4,5] are being investigated. Moreover, those properties have allowed the use of lithium and lithium-based ferrites in applications like memory cores and electromagnetic devices in radio frequency region, since they have high electrical resistivity and frequency-dependent permeability [6–8]. One of the main advantages of these materials is the possibility to control their properties by carefully adjusting their chemical composition and structures [9]. Nowadays, worldwide researchers, are making efforts to analyze different preparation methods and their relation to the macro and microstructure [10–13]. For example, Ramaraghvulu et al. [14] have discussed the analysis of structural, thermal and dielectric studies of Li_2TiO_3. Silva et al. [15] showed the results of the preparation, structural and dielectric property studies of $xLiFe_5O_8$–$(100-x)LiNbO_3$ composite. Chen et al. [16] have reported the results of the thermal measurements, ionic conductivity and dielectric relaxation studies of $LiNaSO_4$. Y.P. Fu and S.H. Hu [17] reported the relationship between the lithium ferrite lattice constant in function of the Mg addition, as a dopant element. In this, the variation of lattice parameters were related with the substitution sites of Mg^{2+}, the relationship between the initial permeability with frequency, determination of Curie temperature via the Arrhenius plots of the electrical conductivity and the microstructure dependence in function of the Mg content. Hankare et al. [18] showed the synthesis of nanoparticles of $Li_{0.5}Fe_{2.5-x}Cr_xO_4$ ferrite system by sol–gel autocombustion method and their structural, magnetic and electrical properties. Abdullah Dar et al. [7] reported the preparation and electrical properties of $Li_{0.5}Al_xFe_{2.5-x}O_4$ ferrite as a function of frequency and composition at room temperature using impedance spectroscopy. Singh et al. [19] showed the dielectric behavior of the zinc substituted *Ni–Mg* ferrites as a cathode material for Li-batteries. The dependence of dielectric properties of Li–Ti ferrites as a function of frequency, composition and temperature has been studied by using impedance measurements

* Corresponding author at: Department of Physics, Federal University of Mato Grosso – UFMT, 78060-900 Cuiabá, MT, Brazil, Tel.: +5565 8115 2400; fax: +5565 3615 8730.
E-mail address: maurocosta@pq.cnpq.br (M.M. Costa).

0925-8388/$ – see front matter © 2011 Elsevier B.V. All rights reserved.
doi:10.1016/j.jallcom.2011.07.038

Table 1
Calcination temperatures for sample preparation.

Sample label	Calcination temperature
LFO-773	773 K
LFO-873	873 K
LFO-973	973 K
LFO-1073	1073 K

in function of the frequency and temperature. The values of electrical conductivity were measured at different temperatures and relaxation time τ was related to the jumping probability.

The study of the electrical conductivity in these materials is important since the associated physical properties like piezoelectricity; pyroelectricity and thermoelectricity are dependent on the nature and the magnitude of the conductivity [20]. It is known that the electric, magnetic and dielectric behaviors depend upon structural properties which are greatly influenced by the preparation method [21,22]. Different methods have been used to prepare lithium ferrite ($LiFe_5O_8$), such as solid-state reaction [23] and conventional ceramic method [24]. Several researchers have studied the frequency and temperature dependence of the dielectric properties of $LiFe_5O_8$ [25–29]. However, there are few studies dealing with the effect of the bindings on the structural and electrical properties of the lithium ferrite ceramic [30]. In this study, $LiFe_5O_8$ ceramics were prepared using the conventional ceramic method. The aim of this paper is to contribute to the understanding the effects of the use of low cost organic bindings, and of the calcination temperature, in the lithium ferrite physical characteristics. Moreover, the effect of the preparation procedure adopted in the structural and electrical properties were examined. The prepared samples structure was characterized by differential scanning calorimetry (DSC), thermogravimetry (TG), X-ray diffraction (XRD) and infra-red spectroscopy (IR). The electric and magnetic properties were investigated using impedance dielectric spectroscopy (IDS) and Mossbauer spectroscopy (MS) techniques, respectively.

2. Experimental procedures

The raw materials used for the preparation of the ferrite samples were high-purity (>99%) oxide (Fe_2O_3) and carbonate (Li_2CO_3), which are commercially available. The bindings analyzed were: bidistilled glycerin (99.5% glycerol); Galactomannan (*Adenanthera pavonina*); PVA (polyvinyl alcohol). These are low cost materials, being one of the main reasons for their choice.

The lithium ferrite ($LiFe_5O_8$–LFO) was prepared by solid state reaction. The precursors powders (Li_2CO_3 and Fe_2O_3) after weighed, in the stoichiometric proportions, were mixed and homogenized in a planetary ball mill system (Fritsch Pulverisette 6), for three hours. Steel balls and steel vessel were used.

The obtained powders were calcinated at temperatures between 773 and 1073 K, for 3 h in air conditions. Table 1 summarizes all the calcinations conditions used.

The LFO powders, calcinated at 1073 K, were mixed with the various bindings. A proportion of 5 and 10%, in weight, of each binder were added to the LFO powder (Table 2) in order to study the effect of the binding content. After a new homogenization process, the composites were pressed in a uniaxial pressure of 1.5 tons using a hydraulic press, at room temperature. The obtained pellets were then sintering in air at 1323 K, for 5 h. After this treatment, all samples present a diameter of 17 mm, approximately, and thickness between 1.5 and 1.8 mm. The heating rate used in the sintering and calcination steps was always of 278 K/min.

The thermal stability of the LFO-binding composites was analyzed by differential scanning calorimetry (DSC) using a Shimadzu DSC-50, in the 303–873 K range. The thermal degradation of the LFO samples was determined by thermogravimetry (TG), using a Shimadzu TGA-50H equipment. The TG thermograms were obtained in the temperature range of 303–1273 K. In both DSC and TG measurements, the samples were sealed in an aluminum cell and heated with a heating rate of 283 K/min, in nitrogen atmosphere.

Table 2
The samples for binding analysis.

Sample label	Binding quantity
LFO-Gly5	Glycerol 5 wt%
LFO-Gly10	Glycerol 10 wt%
LFO-Gal5	Galactomannan 5 wt%
LFO-Gal10	Galactomannan 10 wt%
LFO-PVA5	PVA 5 wt%
LFO-PVA10	PVA 10 wt%

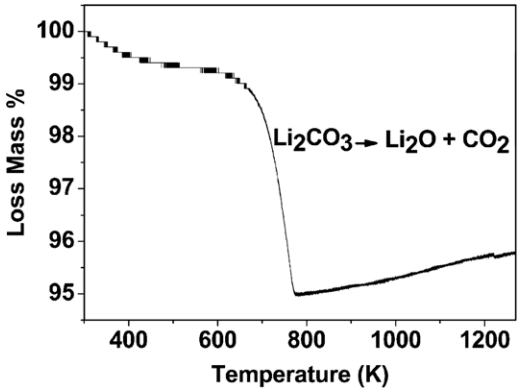

Fig. 1. TG thermograms showing the Li_2CO_3 decomposition.

The formation and preliminary structural properties of the samples were studied by an X-ray diffractometer (Rigaku model D/MAX-B) using Cu Kα radiation and 2θ from 20° to 60° with a scanning rate of 1°/min. The output data extracted from Rietveld refinement was used to calculate the cristallite size [31].

Density measurements using the Archimedes' principle were performed with an ADP 110 balance having a sensitivity of 1 mg. Deionized water was used as liquid for the measurements. The measurements were performed at room temperature (298 K).

The IR spectra of the LFO samples were recorded with a Shimadzu IR spectrophotometer (Model 8300), at room temperature, dry air and between 400 and 800 cm^{-1}. For these measurements, pellets were prepared from the mixture of the samples powder with KBr in the proportion of 1:200 (wt).

The dielectric measurements, performed in the temperature range between 303 and 383 K, were performed using a Solartron 1260 impedance analyzer. The electrodes were prepared by applying a thin layer of silver conductive paint on the opposite surfaces of the disk shape samples. During the experience and at each temperature of measurement, a period of 25 min was used before the data acquisition, in order to ensure stable thermal conditions and therefore improve the accuracy of the measurement.

The Mossbauer spectra were measured at room temperature in standard transmission geometry, using a constant acceleration spectrometer with a radioactive source of ^{57}Co in an Rh matrix at 298 K. The spectra of the lithium ferrite ceramic matrix (LFO) were evaluated using the fitting software Normos. Values of the isomer shift (δ) quoted are relative to metallic iron (α-Fe). The ^{57}Fe Mössbauer spectroscopy was performed with Fast Comtec spectrometer model MR-351.

3. Results and discussion

3.1. Differential scanning calorimetry (DSC) and thermogravimetry (TG)

Figs. 1 and 2 present the TG and DSC thermograms, respectively. The TG curve (Fig. 1) revealed a sharp mass loss between 673 and 773 K, related with the decomposition of Li_2CO_3 in Li_2O and CO_2 [26,27].

The DSC curve (Fig. 2) shows two endothermic transitions, the first at 474 K, which is associated with the organic weight losses and the second at 831 K indicating the complete thermal decomposition of Li_2CO_3.

3.2. XRD analysis

Fig. 3 shows the XRD patterns of the LFO samples calcinated between 773 and 1073 K (LFO-773, LFO-873, LFO-973 and LFO-1073). As one can see, the calcination at 773 K does not promote the total formation of lithium ferrite. Moreover, the Rietveld refinement results confirm that the spinel cubic structure of the samples calcinated at 873 K is not yet complete, whereas for the samples calcinated at higher temperatures, LFO-973 and LFO-1073, the spinel

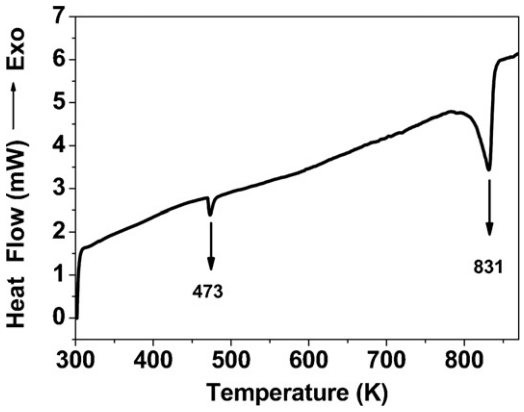

Fig. 2. DSC thermograms of the formation of the $LiFe_5O_8$.

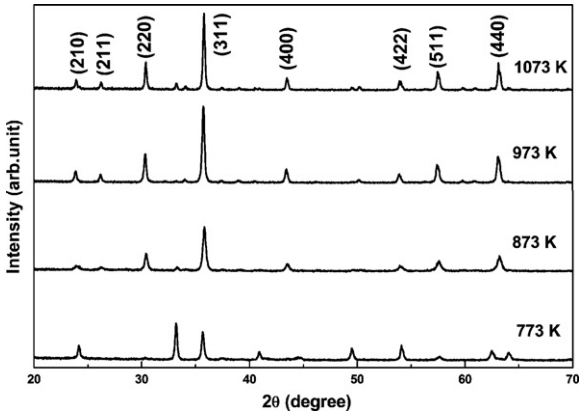

Fig. 3. XRD patterns of the $LiFe_5O_8$ samples for various calcination temperatures.

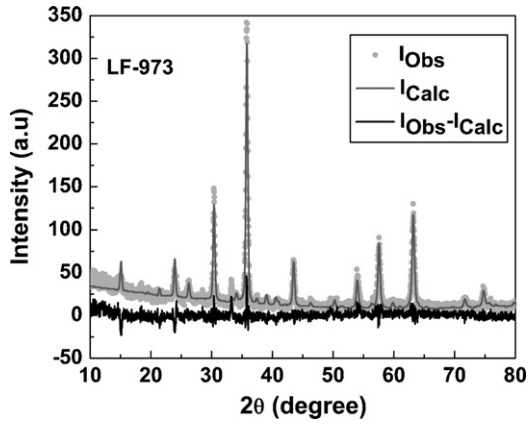

Fig. 4. XRD patterns of the LFO-973 sample. Circle symbol as experimental data, line as calculated data and difference at bottom.

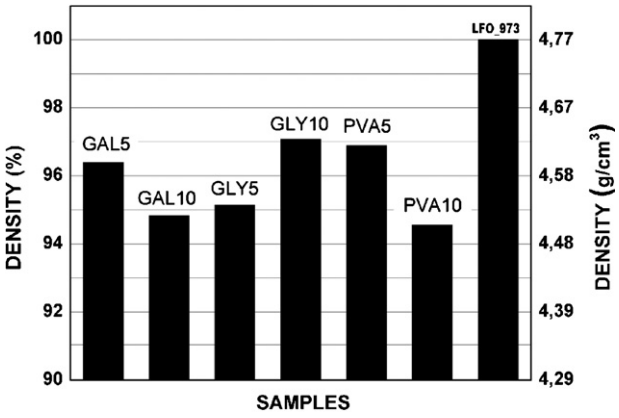

Fig. 5. Experimental densities.

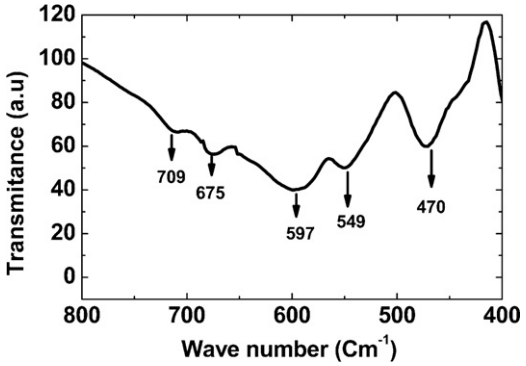

Fig. 6. Infrared spectrum of the $LiFe_5O_8$.

structure is obtained. Table 3 summarizes these results. In this table, the number in parentheses, after the average particle size, refers to the experimental error. A graphical example of the Rietveld refinement for sample LFO-973 is plotted in Fig. 4. The average of the calculated density for the samples LFO-873/973/1073 was 4.769 g/cm^3. As expected for the average particle size of each family of crystalline plans, it increases with the increase of the temperature of calcination, in a range from 1 to 15 nm for every 373 K increment.

The densities of the samples presented in Table 2 (LFO powders mixed with different bindings) were measured by Archimedes method and the results are shown in Fig. 5. The last column represents the density evaluated from the Rietveld Refinement of LFO-973 sample (4.77 g/cm^3). It can be observed that the lower and higher densities values were found for LFO-PVA10 (4.51 g/cm^3) and LFO-Gly10 (4.63 g/cm^3), respectively. Due to the high value of the obtained density and the lower cost, the glycerol seems to be a good option as a binder.

3.3. Infrared spectra

The infrared spectroscopy was used to investigate the sample structure. Fig. 6 shows the transmittance spectrum, which shows bands centered at 470, 549, 597, 675 and 709 cm^{-1}, which are

Table 3
Rietveld refinement data.

Samples	Average crystallite size (nm)	Phase	Density (g/cm^3)	Lattice parameters
LFO-773	41.6 (3)	$Li_2Fe_2O_4$	4.377	$a=b=4.0505$ Å $c=8.7694$ Å $\alpha=\beta=90^\circ$, $\gamma=120^\circ$
LFO-873	27.9 (4)	SPINEL $LiFe_5O_8$	4.769	$a=b=c=8.3251$ Å $\alpha=\beta=\gamma=90^\circ$
LFO-973	37.9 (2)	SPINEL $LiFe_5O_8$	4.769	$a=b=c=8.3253$ Å $\alpha=\beta=\gamma=90^\circ$
LFO-1073	53.8 (4)	SPINEL $LiFe_5O_8$	4.768	$a=b=c=8.3257$ Å $\alpha=\beta=\gamma=90^\circ$

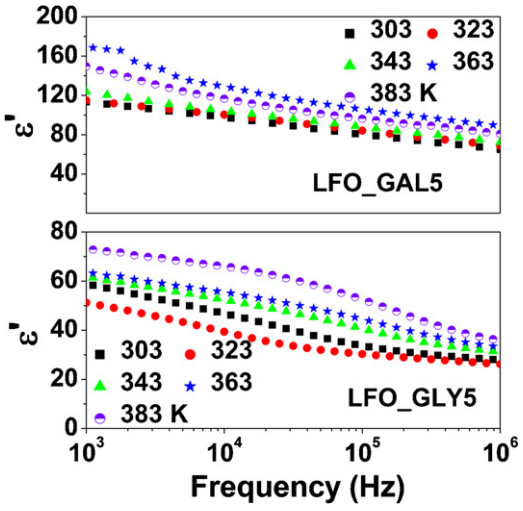

Fig. 7. ε' vs. frequency at different temperature LFO-Gal5 and LFO-Gly5.

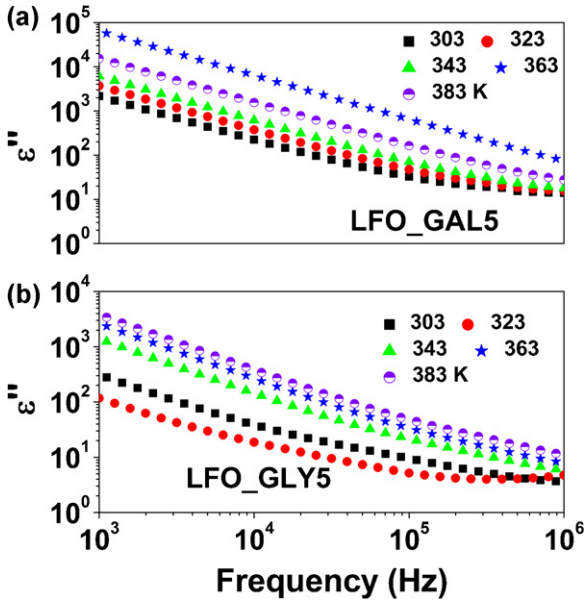

Fig. 8. ε'' vs. frequency at different temperature (a) LFO-Gal5 and (b) LFO-Gly5.

characteristic of the α-$LiFe_5O_8$ (ordered) phase [25]. The bands in the range 549–597 cm^{-1} are due to the scratching vibrations metal–oxygen (Fe–O) bond on tetrahedral sites (ν_A) and the band at 470 is assigned to metal–oxygen (Fe–O) vibrations in octahedral sites (ν_B) [29,32]. The infrared spectrum was made only for the lithium ferrite samples calcinated at 973 K and 1073 K. No significant differences were observed in the spectra for different temperatures.

3.4. Dielectric spectroscopy

The dielectric response is one of the most important properties of ferrites, which markedly depend on the preparation conditions, e.g. sintering time, temperature, type and quantity of additives. The study of the dielectric properties produces valuable information on the behavior of localized electric charge carriers [33–35] leading to better understanding of the dielectric polarization mechanism in these prepared samples. Generally, the complex relative permittivity ε^* of materials is defined by $\varepsilon^*(\omega) = \varepsilon' - j\varepsilon''$. In this work, the dielectric measurements were performed in the samples with 5 wt% of Galactomannan (LFO-Gal5) and with 5 wt% of glycerol (LFO-Gly5).

The variation of the dielectric constant (ε') with frequency for LFO-Gal5 and LFO-Gly5 at different temperatures is shown in Fig. 7. It was found that in the range between 1 kHz and 1 MHz the ε' value decreases considerably, for all samples, with the increase of the frequency and that the samples containing Gal present a value of ε' higher than the samples containing Gly. It is known that the polarization in ferrites is mainly through a mechanism similar to the conduction process, by electron exchange between Fe^{2+} and Fe^{3+}, one obtains local displacement of electrons in the direction of the applied field and these electrons determine the polarization. The polarization decreases with increase in frequency is due to the fact that, beyond a certain frequency of external field, the electronic exchange between Fe^{2+} and Fe^{3+} cannot follow the alternating field decreasing their contribution to the system polarizability [21]. According to Fig. 7, ε' increases with the rise of the measuring temperature indicating a thermal activated process.

The variation of the imaginary part of the dielectric permittivity (ε'') with frequency, at different temperatures are shown in Fig. 8. This figure reveals that ε'' decreases with increasing frequency and that the value for the sample LFO-GAL5 is higher than the value for the sample with glycerol, in all the frequency range. It must be noticed that for measuring temperatures above 363 K the dielectric behavior between both bindings becomes the opposite (Figs. 7 and 8). The occurrence of this behavior modification can be related with a phase transition, in this temperature range [36]. There are no appreciable relaxation peaks in the frequency range used in this study. The dielectric loss rise sharply at low frequency indicating that electrode polarization and space charge effects have occurred confirming a non-Debye dependence [33,37,38].

According to Fig. 9, ε' depends on temperature and frequency, and increases with increasing temperature. The value of the dielectric constant temperature at 303 K for the sample containing Gal, is twice the value obtained for sample with Gly, which indicates a strong effect of the Gal binding in the dielectric constant behavior. The variation of dielectric constant with temperature for the samples with Gly is lower when compared with the sample containing Gal, in the same temperature range.

Fig. 10 shows a strong dependence between ε'' and temperature in the frequency range of 100 Hz to 1 kHz. The values of ε'' of the samples with Gal are always the lowest. Therefore the dielectric loss, which increases with increasing temperature and decreases with increasing frequency, presents the lowest value for the sample containing Gly [30].

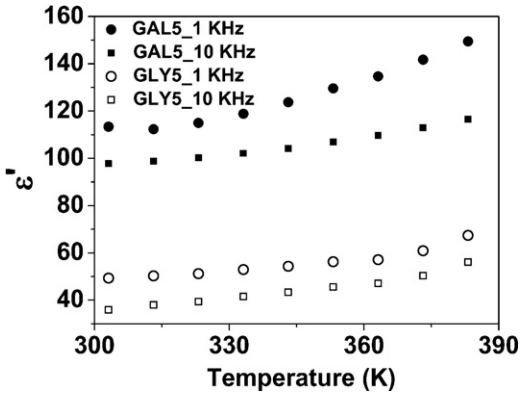

Fig. 9. Temperature dependence of ε' at different frequencies.

Table 4
^{57}Fe Mössbauer parameters recorded at 298 K temperature from mixture of Li_2CO_3 and Fe_2O_3 (LFO-298), calcinated $LiFe_5O_8$ (LFO-1073) and sinterized $LiFe_5O_8$ (LFO-1323).

Samples	Subspectrum	δ (mm s^{-1}) (±0.01)	Δ (mm s^{-1}) (±0.01)	H_{hf} (T) (±0.1)	Area (%)
LFO-298	Sextet	0.37	−0.14	51.9	98
	Doublet	0.36	0.47	–	2
LFO-1073	Sextet A	0.32	−0.020	52.3	50
	Sextet B	0.30	0.000	50.3	50
LFO-1323	Sextet A	0.32	0.00	51.8	59
	Sextet B	0.31	0.592	44.09	41

3.5. Mössbauer spectroscopy

The room temperature Mössbauer hyperfine parameters such as quadrupole splitting (Δ), isomer shift (δ), magnetic hyperfine field (H_{hf}) and the relative area (%) have been determined from the analysis of the spectra and tabulated in Table 4. The analysis of the Mössbauer spectra provides important information about their chemical, structural and magnetic properties. Spinel type lithium ferrites ($LiFe_5O_8$) are composed of two six-line hyperfine patterns. It occurs in two crystalline forms: ordered and disordered structures. In the ordered form (α-phase) the Fe^{3+} ions are at octahedral 12d sites (B-site) and tetrahedral 8c sites (A-site), and Li^{1+} ion occupy only the octahedral 4b sites in the cubic primitive unit cell. In the disordered form, β-$LiFe_5O_8$ has an inverse spinel structure, with Fe^{3+} at tetrahedral 8a positions and Li^{1+} and Fe^{3+} randomly distributed over the 16d octahedral site [22,39–41].

A simple fitting model to ^{57}Fe Mössbauer spectrum of the lithium ferrite ceramic matrix ($LiFe_5O_8$) (Fig. 11) was adopted with two overlapping sextets, A and B, for the octahedral and tetrahedral sites.

The analyzed samples were labeled as LFO-298, LFO-1073 and LFO-1323. LFO-298 is made of a simple mixture of raw powder, LFO-1073 represents the calcinated powder at 1073 K and LFO-1323 is a platelet sinterized at 1323 K.

The spectra of LFO-298 was adjusted by a magnetic sextet for the site of hematite and the spectra LFO1073 was adjusted for two magnetic sextet attributed to Fe^{3+} ions referring to sites tetrahedral (A) and octahedral (B) Li of the ferrite with low hyperfine magnetic fields (~52.3 T and 50.3 T) for fields of characteristic of $LiFe_5O_8$ and the spectra LFO-1323 were adjusted by two magnetic sextet in the tetrahedral site (A) and octahedral (B) of the $LiFe_5O_8$ with low hyperfine magnetic fields (~51.8 T and 44.9 T) [42]. In this paper we did not measure the magnetic hysteresis characteristics of the samples.

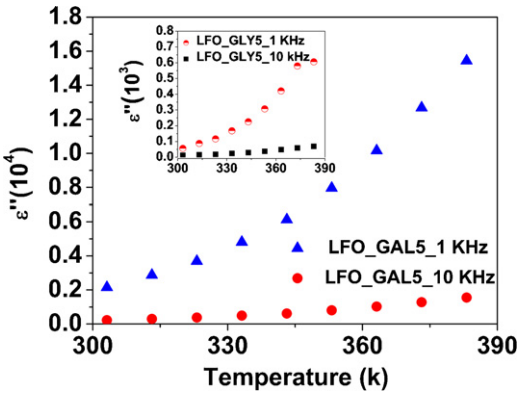

Fig. 10. Temperature dependence of ε'' at different frequencies.

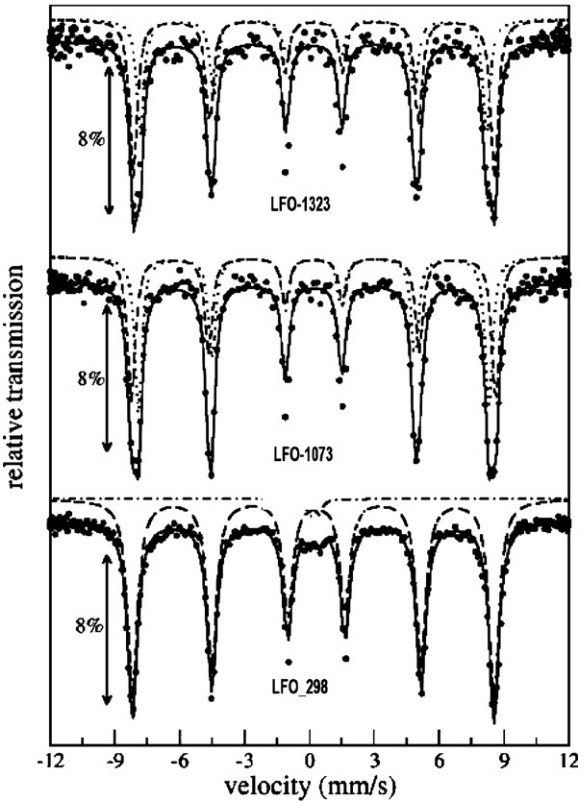

Fig. 11. ^{57}Fe Mössbauer spectrum recorded from the noncalcinated mixture of Li_2CO_3 and Fe_2O_3 (LFO-298), a calcinated mixture at 1073 K (LFO-1073) and a pellet sinterized at 1323 K (LFO-1323).

4. Conclusions

In this paper, we investigate the effects of the calcination temperature and the organic bindings in the structural and dielectric properties of lithium ferrite ($LiFe_5O_8$). The used bindings were glycerol, PVA (Polyvinyl alcohol) and Galactomannan (*A. pavonina*). The investigated calcination temperature was varied from 773 up to 1073 K. The use of different bindings produced samples with almost identical densities, but with different electrical characteristics as showed by the permittivity and dielectric loss. These results show that the organic bindings significantly alter the relative permittivity and dielectric loss. The increase of ε' with increasing temperature is attributed to the decrease in polarization time. The enhanced electrical conductivity makes a major contribution to the increase of ε'' with increasing temperature. The spinel structure was identified by Mössbauer and thermal analyzes. The complete thermal decomposition of Li_2CO_3 was established by the DSC and TG techniques pointing out the decomposition of Li_2CO_3 between 773 and 831 K. The study of the structural and electrical properties of lithium ferrites is important in view to their attractive technological properties and low cost of fabrication.

Acknowledgements

The authors thank to the Prof. Dr. Ricardo Emílio Quevedo Ferreira Nogueira (Biomaterials, Federal University of Ceará – Brazil), for the use of theirs laboratories for samples preparation, Prof. Dr. Igor Vasconcelos (Federal University of Ceará – Brazil) for the Mössbauer spectroscopy and *RENORBIO* Pos-Graduation Programme beyond Brazilian funding agency by *CNPq*, *FAPEMAT* and *FUNCAP*. MMC thanks H. Blas for reading the manuscript and suggestions.

References

[1] H. Maa, Z. Yuana, F. i Chenga, J. Lianga, Z. Tao, J. Chena, J. Alloys Compd. 509 (20) (2011) 6030–6035.
[2] A.N. Jansena, J.A.M. Baeblera, J.T. Vaughey, J. Alloys Compd. 509 (13, 31) (2011) 4457–4461.
[3] Y. Sakurai, H. Arai, J. Yamaki, Solid State Ionics 29 (1998) 113–115.
[4] V. Verma, V. Pandey, R.K. Kotnala, H. Kishan, N. Kumar, P.C. Kothari, J. Alloys Compd. 443 (1–2) (2007) 178–181.
[5] L. Fang, D. Chu, H. Zhou, X. Chen, Z. Yang, J. Alloys Compd. 509 (5) (2011) 1880–1884.
[6] M. Naoe, R. Takahashi, T. Omura, Y. Hotta, T. Sato, K. Yamasawa, Y. Miura, J. Magn. Magn. Mater. 320 (20) (2008) 949–953.
[7] M. Abdullah Dara, Khalid Mujasam Batoob, Vivek Vermac, W.A. Siddiquia, R.K. Kotnala, J. Alloys Compd. 493 (1–2) (2010) 553–560.
[8] T. Nakamura, M. Naoe, Y. Yamada, J. Magn. Magn. Mater. 305 (1) (2006) 120–126.
[9] S.A. Patil, V.C. Mahajan, M.G. Patil, A.K. Ghatage, S.D. Lotke, J. Mater. Sci. 34 (1999) 6081–6086.
[10] S.F. Mansour, M.A. Elkestawy, Ceram. Intern. 37 (2011) 1175–1180.
[11] K. Niesz, T. Ould-Ely, H. Tsukamoto, D.E. Morse, Ceram. Intern. 37 (2011) 303–311.
[12] S.K. Rout, S. Parida, E. Sinha, P.K. Barhai, I.W. Kim, Curr. Appl. Phys. 10 (2010) 917–992.
[13] H. Singh, A. Kumar, K.L. Yadav, Mater. Sci. Eng. B 176 (2011) 540–547.
[14] R. Ramaraghavulu, S. Buddhudu, G.B. Kumar, Ceram. Intern. 37 (2011) 1245–1249.
[15] C.C. Silva, D.X. Gouveia, M.P.F. Graça, L.C. Costa, A.S.B. Sombra, M.A. Valente, J. Non-Cryst. Solids 356 (2010) 602–606.
[16] R.H. Chen, C.M. Tseng, C.S. Shern, T. Fukami, Solid State Ionics 181 (2010) 877–882.
[17] Y.P. Fu, S.H. Hu, Ceram. Intern. 36 (2010) 1311–1317.
[18] P.P. Hankare, R.P. Patil, U.S. Sankpal, K.M. Garadkar, R. Sasikala, A.K. Tripathi, I.S. Mulla, J. Magn. Magn. Mater. 322 (2010) 2629–2633.
[19] N. Singh, A. Agarwal, S. Sanghi, Curr. Appl. Phys. 11 (2011) 783–789.
[20] H.M. Zaki, J. Alloys Compd. 439 (2007) 1–8.
[21] R.R. Heikes, W.D. Jonston, J. Chem. Phys. 26 (1957) 582–587.
[22] A. Tomas, P. Laruelle, J.L. Dormann, M. Nogues, Acta. Crystallogr. Sect. C: Cryst. Struct. Commun. 39 (1983) 1615–1617.
[23] S. Kumar, R.K. Alimuddin, P. Thakur, K.H. Chae, B. Angadi, W.K. Choi, J. Phys. Condens. Matter 19 (2007) 1–15.
[24] A.M. Samya, A.A. Sattara, I.H. Afify, J. Alloys Compd. 505 (1) (2010) 297–301.
[25] K.V. Kumar, A.C.S. Reddy, D. Avinder, J. Magn. Magn. Mater. 263 (2003) 121–126.
[26] A.M. Abo El Atta, S.M. Attia, J. Magn. Magn. Mater. 257 (2003) 165–174.
[27] A.M. Abo El Atta, M.A. Ahmed, J. Magn. Magn. Mater. 208 (2000) 27–36.
[28] A.M. Abo El Atta, E. Hiti, J. Phys. III (France) 7 (1997) 883–894.
[29] N. Rezlescu, E. Rezlescu, Phys. Stat. Sol. A 23 (1974) 575–582.
[30] R.S.T.M. Sohn, A.A.M. Macêdo, M.M. Costa, S.E. Mazzetto, A.S.B. Sombra, Phys. Scr. 82 (2010) 055702.
[31] C.C. Silva, M.P.F. Graça, M.A. Valente, A.S.B. Sombra, J. Mater. Sci. 42 (11) (2007) 3851–3855.
[32] R.D. Waldron, Phys. Rev. 99 (1955) 1727–1735.
[33] M.M. Costa, G.F.M. Pires Júnior, A.S.B. Sombra, Mater. Chem. Phys. 123 (2010) 35–39.
[34] M.S. Cao, Z.L. Hou, J. Yuan, L.T. Xiong, X.L. Shi1, J. Appl. Phys. 105 (2009) 106102–106103.
[35] M.S. Cao, W.L. Song, Z.L. Hou, B. Wen, J. Yuan, Carbon 48 (2010) 788–796.
[36] F.M.M. Pereira, M.R.P. Santos, R.S.T.M. Sonh, J.S. Almeida, A.M.L. Medeiros, M.M. Costa, A.S.B. Sombra, J. Mater. Sci. Mater. Electron. 20 (2009) 408–417.
[37] X. Qian, N. Gu, Z. Cheng, X. Yang, S. Dong, Electrochim. Acta 46 (2001) 1829–1836.
[38] G. Govindaraj, N. Baskaran, K. Shahi, P. Monoravi, Solid State Ionics 76 (1995) 47–55.
[39] E. Wolska, P. Piszora, W. Nowicki, J. Darul, Int. J. Inorg. Mater. 3 (2001) 503–507.
[40] H.M. Widatallah, F.J. Berry, J. Solid State Chem. 164 (2002) 230–236.
[41] S.Y. An, I.B. Shim, C.S. Kim, J. Magn. Magn. Mater. 290–291 (2005) 1551–1554.
[42] R.G. Gupta, G.R. Mendiratta, J. Appl. Phys. 48 (7) (1977) 2998–3001.